Dielectric Studies of a Substance with Negative Dielectric Anisotropy

S. Urban, B. Gestblom^a, R. Dąbrowski^b, and H. Kresse^c

Institute of Physics, Jagellonian University, Reymonta 4, 30-059 Cracow, Poland

^a Institute of Physics, Uppsala University, S-75121 Uppsala

b Institute of Chemistry, Military Academy of Technology, Warsaw, Poland Institute of Physical Chemistry, Martin Luther University, Halle/S., Germany

Z. Naturforsch. 53a, 134-140 (1998); received February 20, 1998

The results of dielectric studies of 6BAP(F) (1-[4-(hexylbicyclo[2,2,2]octyl]-2-(3-fluoro-4-methoxyphenyl)ethane) in the nematic and isotropic phases are presented. The substance has a negative dielectric anisotropy. By applying two experimental techniques, using a network analyzer and time domain spectrometer (TDS), the two main relaxation processes, connected with the molecular reorientation around the short and long axes, respectively, were resolved in the phases studied. The activation barriers hindering the motions were obtained. By extrapolation of the longitudinal and transverse relaxation times from the isotropic to the nematic phase the retardation factors, g_{\parallel} and g_{\perp} , and the nematic potential versus temperature could be calculated. These are discussed together with the order parameter S obtained from the refractive index, and are compared with the predictions of the mean-field theories.

Key words: Liquid Crystals, Dielectric Anisotropy, Dielectric Relaxation, Retardation Factors.

1. Introduction

The dielectric properties of liquid crystalline (LC) substances change drastically when the nematic – isotropic (N – Is) transition point is crossed. The static permittivity, ε_s , is a tensorial quantity in the N phase with two components, $\varepsilon_{s\parallel}$ and $\varepsilon_{s\perp}$, corresponding to the appropriate alignment of the director n with respect to the measuring electric field E ($E \parallel n$ and $E \perp n$, respectively). The dielectric anisotropy $\Delta \varepsilon = \varepsilon_{\parallel} - \varepsilon_{\perp}$, dependends on the value and the direction of the dipole moment with respect to the long molecular axis. In the isotropic phase, ε_{is} is comparable with the mean value $\bar{\varepsilon} = (\varepsilon_{s\parallel} + 2 \varepsilon_{s\perp})/3$. Also the molecular dynamics changes considerably at the clearing point due to the disappearance of the nematic potential. This especially concerns the rotation of molecules around their short axes (observed as ε^* (v) relaxation at MHz frequencies, the low frequency, l.f., process). On the other hand, the rotation around the long axis (observed as ε^* (v) relaxation at GHz frequencies, the high frequency, h.f., process) is believed to be even facilitated in the presence of the nematic potential [1–5]. However, the experimental evidence concerns mainly the l.f. process (eg. [6–10]), whereas the h.f. one was studied for a rather limited number of substances [9–12].

We have performed dielectric studies of 1-(4-(hexylbicyclo[2,2,2]octyl]-2-(3-fluoro-4-methoxyphenyl)-

which can be compared with 1-(4-isothiocyanatophenyl)-2-(4-hexyl-bicyclo[2,2,2]octane-1)ethane (6BAPT),

$$H_{13}C_6$$
 — CH_2CH_2 — NCS ,

recently studied by Jadzyn et al. [10]. Due to the fluorine atom at the orto-position of the benzene ring, 6BAP(F) has a larger transverse than longitudinal components of the dipole moment, contrary to 6BAPT, having a strong longitudinal dipole moment. Appropriate orientation of the nematic sample by a magnetic field $(E \parallel B, \text{ or } E \perp B)$ and use of two set-ups (impedance analyzer and time domain spectrometer – TDS) enabled us to detect both main relaxation processes connected with the molecular reorientations around the short and the long axes. With the TDS spectrometer covering a broad frequency range (10 MHz – 5 GHz), we believed that the above motions could also be separated in the isotropic phase of 6BAP(F). This was really the case, and the measured spectra allowed for a clear separation of the two relaxation processes.

Thus, we could obtain two sets of relaxation times: τ_{\parallel} and τ_{\perp} in the nematic phase τ_{l} and τ_{t} in the isotropic

Reprint requests to Prof. S. Urban; Fax: 0048-12-6337086.

phase of 6BAP(F). This leads to the definition of two retardation factors $g_{\parallel} = \tau_{\parallel}/\tau_{\parallel}$ and $g_{\perp} = \tau_{\perp}/\tau_{\parallel}$, which characterize the same molecular motions with and without the nematic potential, This is a refinement to the use of the so-called 'Debye relaxation time $\tau_{\rm D}$ ' commonly employed in the theoretical papers [1–4] for the characterization of the relaxation process in the isotropic phase. However, in a recent paper by Kalmykov and Coffey [5] the above definitions were introduced and interesting relationships were obtained. We shall discuss the present results in relation to the predictions of the mean-field theories [1–5].

Experimental

The substance was synthetized as described in [13]. Its transition temperatures were: Cr-58.9 °C-N-65.6 °C-Is; however, the nematic phase could be easily supercooled below 40 °C.

The measurement of $\varepsilon^*(v) = \varepsilon'(v) - i \varepsilon''(v)$ for the nematic phase was performed in the frequency range of 1 kHz - 13 MHz using a HP 4192 A impedance analyzer. A parallel-plate capacitor ($C_0 = 7 \text{ pF}$) was calibrated using standard liquids. The sample was oriented by a magnetic field of 0.6 T. The measurements of \mathcal{E}_{is}^* in the isotropic phase and ε_{\perp}^* in the nematic phase were performed with the aid of the time domain spectroscopy technique (TDS). For the experimental details see [8, 9, 14]. In the case of the isotropic phase, three time windows were used (10 ns, 50 ns, and 100 ns) and then the spectra were spliced as described in [9]. This allowed for covering the frequency range from 10 MHz to ca. 3 GHz. The perpendicular orientation was obtained by applying a magnetic field of about 0.5 T. These spectra were collected with two time windows (10 ns and 50 ns).

The refractive index measurements were performed using an Abbé refractometer. A homeotropic orientation of the sample was obtained by covering of a glass surface by an alcoholic solution of hexadecyltrimethylammonium bromide.

Results

The dielectric spectra, measured in different phases of 6BAP(F) and presented in the form of Cole-Cole plots ε'' vs. ε' , are shown in Figure 1. The particular spectra were analyzed with the well known Cole-Cole equation

$$\frac{\varepsilon^*(\omega) - \varepsilon_{\infty}}{\varepsilon_{s} - \varepsilon_{\infty}} = \frac{1}{1 + (i\omega\tau)^{1-\alpha}},\tag{1}$$

where $\varepsilon_{\rm s}$ and $\varepsilon_{\rm \infty}$ are the static and high frequency permittivities, respectively, and α characterizes the distribution of relaxation times.

As is seen in Fig. 1a, the spectrum of the isotropic phase of 6BAP(F) shows two bands which can be attributed to the molecular reorientations around the short axis (l.f. band) and around the long axis (h.f. band). In order to separate the two processes we used a superposition of two Debye equations,

$$\varepsilon_{is}^{*}(\omega) - \varepsilon_{is\infty} = \frac{\delta_{1}}{1 + i \omega \tau_{1}} + \frac{\delta_{t}}{1 + i \omega \tau_{t}},$$
 (2)

where the subscripts l and t correspond to the longitudinal and transverse components of the dipole moment, and $\delta_l = \varepsilon_{is,l} - \varepsilon_{is,t}$, $\delta_t = \varepsilon_{is,t} - \varepsilon_{is,\infty}$, are the strengths (increments) of these relaxation processes. The fitting parameters of (2) are presented in Figs. 2 and 3. The activation barriers calculated for the particular relaxation processes are listed in Table 1.

In the case of $E \parallel B$ geometry we are dealing with a single relaxation process, well described by the Debye equation ($\alpha = 0$ in (1)) with τ_{\parallel} and $\varepsilon_{\parallel \infty}$ as fitting parameters (see Figure 1b). However, the $\varepsilon_{\parallel}^*$ spectra above ca. 7 MHz were desturbed by the second relaxation process which was not studied here. The permittivities $\varepsilon_{\rm s\parallel}$ and $\varepsilon_{\parallel \infty}$ obtained for different temperatures are shown in Fig. 2, whereas the relaxation times in the form of the Arrhenius plot are presented in Figure 3. For the $E \perp B$ geometry the spectra exhibit a small distribution of τ_{\perp} with $\alpha \approx 0.05 \div 0.10$ (Figure 1b). The fitting parameters of (1) are presented in Fig. 2 ($\varepsilon_{\rm s\perp}$ and $\varepsilon_{\perp \infty}$) and Fig. 3 (τ_{\perp}). The $\varepsilon_{\rm s\perp}$ -values obtained from both experimental methods agree well.

Figure 4 shows the refractive index data for the isotropic and nematic phase of 6BAP(F). It is characteristic that in the nematic phase the mean value $\bar{n} = (n_e + 2 n_0)/3$

Table 1. Parameters of the Arrhenius equation $\tau=\tau_0$ exp (Δ H/RT) for the different relaxation processes observed in the nematic and isotropic phases of 6BAP(F). The activation barriers calculated from the results of paper [10] for the similar substance 6BAPT are also listed.

Phase	Relaxation process	$ au_0$ s	∆H kJ/mol	ΔH (6BAPT) kJ/mol
Nematic	<u> </u>	$1.02 \times 10^{-19} \\ 4.19 \times 10^{-15}$	73.4±2 30.0±2	75.9
Isotropic	l t	$2.44 \times 10^{-17} \\ 4.33 \times 10^{-14}$	55.0 ± 3 23.6 ± 2	24.4

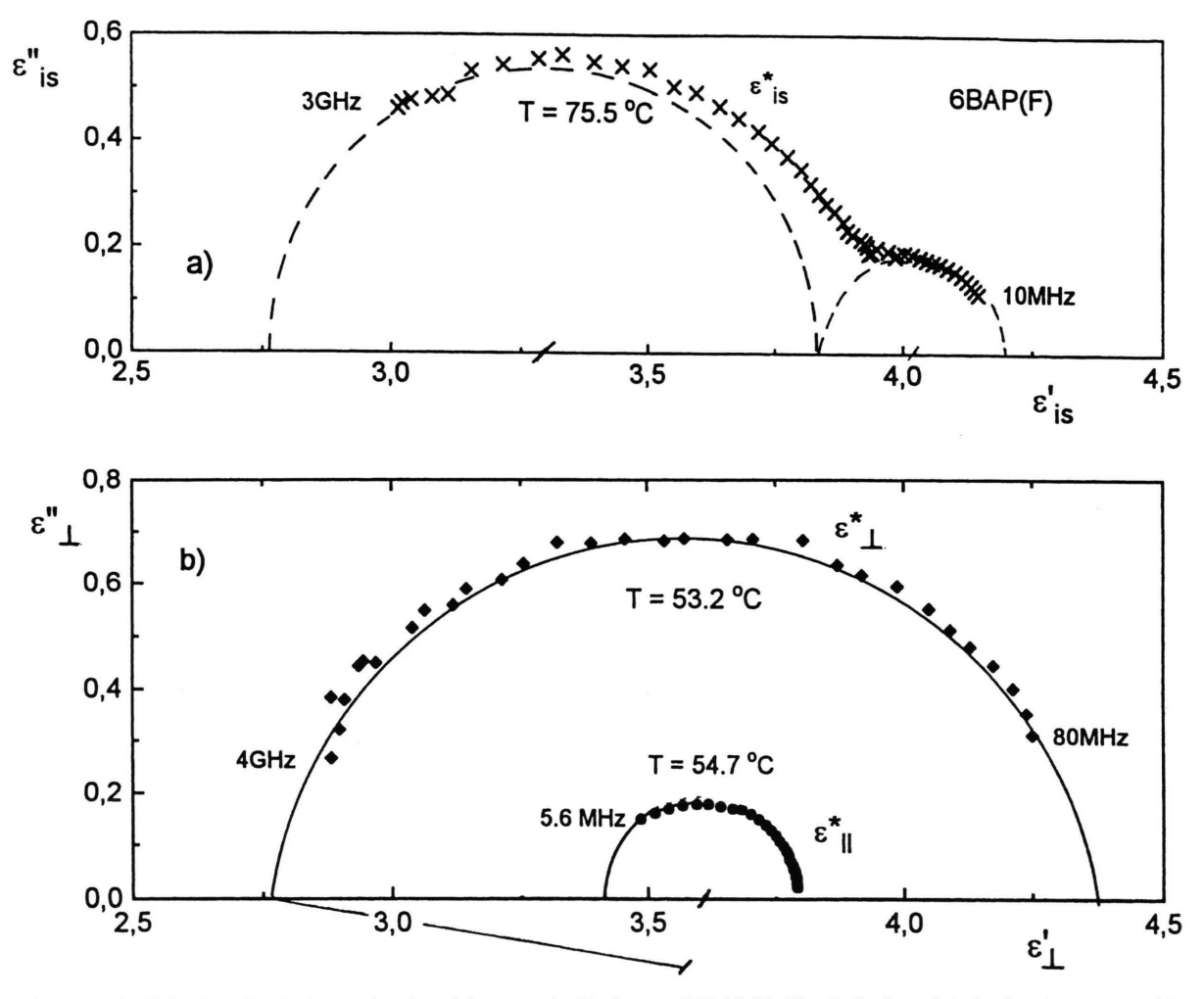


Fig. 1. Cole-Cole plots for the isotropic (a) and the nematic (b) phases of 6BAP(F). The dashed semicircles in (a) correspond to two Debye-type processes according to [2], the solid circles in (b) correspond to [1].

is greater than the extrapolated $n_{\rm is}$ -values. The optical anisotropy $\Delta n = n_{\rm e} - n_0$ enables one to calculate the order parameter S [15]. For this purpose we applied the method proposed by Horn [16], who adopted the well known Haller formula $S = (1 - T/T_{\rm NI})^{\gamma}$. From the plot of $\lg \Sigma$ versus $\lg (1 - T/T_{\rm NI})$ (where $\Sigma = (n_{\rm e}^2 - n_0^2)/(\tilde{n}^2 - 1)$) the exponent $\gamma = 0.128$ and the scaling factors, $0.238 = \Sigma /S$ or $0.0991 = \Delta n/S$, were obtained. Figure 5 presents the fit of the Haller equation to the experimental points. Because in many NMR experiments (eg. [17]) the order parameter S reaches smaller values close to the clearing temperature $T_{\rm NI}$ (ca. 0.32), the present data may be overestimated by a factor of ca. 1.3.

Discussion

6BAP(F) has a negative dielectric anisotropy, $\Delta \varepsilon = \varepsilon_{s\parallel} - \varepsilon_{s\perp}$, as is seen in Figure 2. Taking into consideration the Maier-Meier equation [18]

$$\Delta \varepsilon = \varepsilon_{\text{lls}} - \varepsilon_{\perp s} = N \frac{h F}{\varepsilon_0} \left[\Delta \alpha - F \frac{\mu^2}{2 k_B T} \times (3) \right]$$

$$(1 - 3 \cos^2 \beta) S,$$

one can conclude that the dipole moment μ is directed at an angle $\beta > 54^{\circ}$ with respect to the long molecular axis, as the polarizability anisotropy $\Delta \alpha$ must be positive for

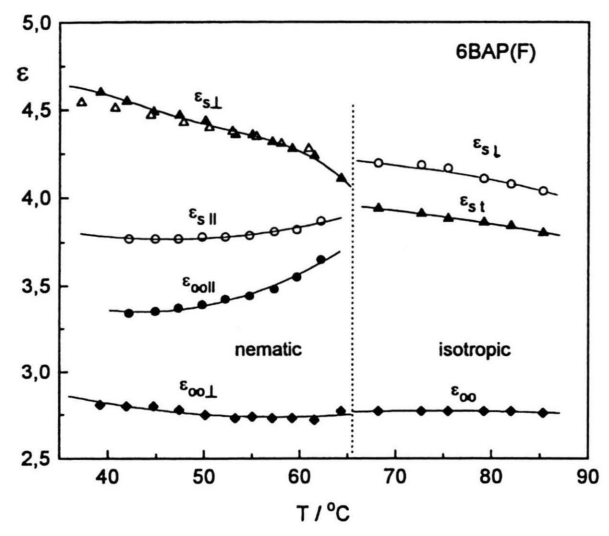


Fig. 2. Permittivity values vs. temperature obtained from the analysis of the spectra with the aid of (1) and (2).

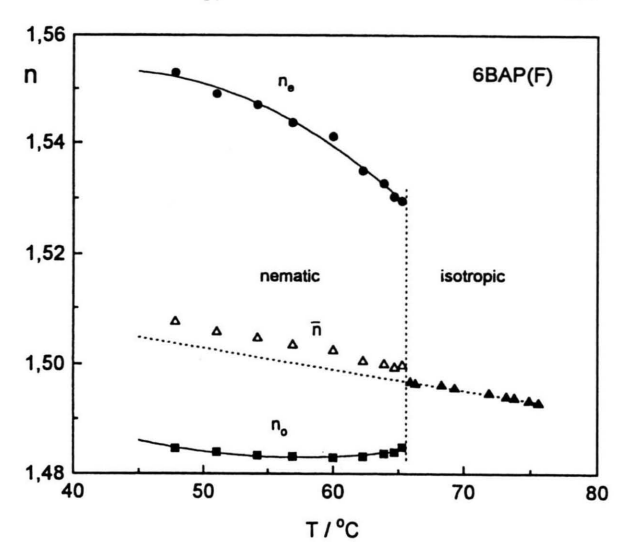


Fig. 4. Refractive indices vs. temperature for the nematic and isotropic phases of 6BAP(F).

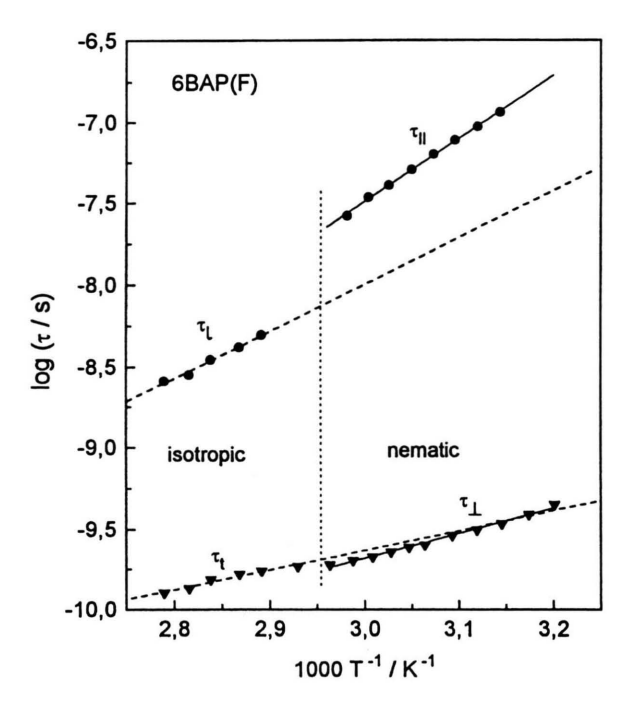


Fig. 3. Arrhenius plots for the nematic and isotropic phases of 6BAP(F).

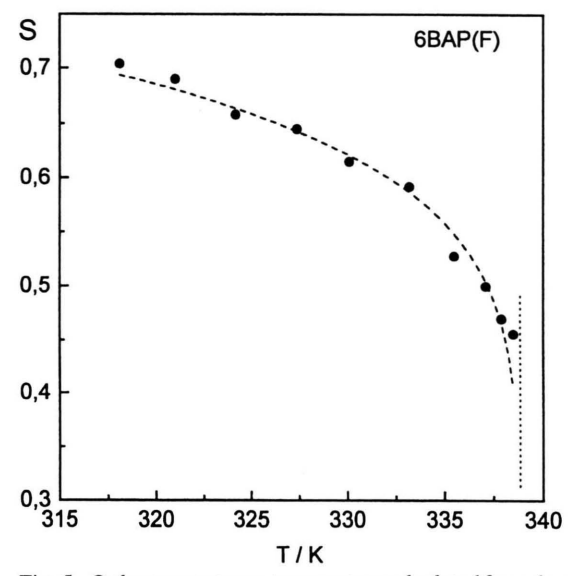


Fig. 5. Order parameter vs. temperature calculated from the optical anisotropy data. The dashed line corresponds to the Haller equation (see text).

rod-like molecules (h and F are the local field factors depending on the average permittivity, N is the number of molecules per unit volume, S the order parameter and ε_0 the free space permittivity). The angle β can be estimated from the dielectric increments δ_1 and δ_t for the iso-

tropic phase using the Onsager equation,

$$\mu^{2} = \frac{9 k_{B} T \varepsilon_{0} (\varepsilon_{s} - \varepsilon_{\infty}) (2 \varepsilon_{s} - \varepsilon_{\infty})}{N \varepsilon_{s} (\varepsilon_{\infty} + 2)^{2}},$$
 (4)

separately for the two components of the dipole moment.

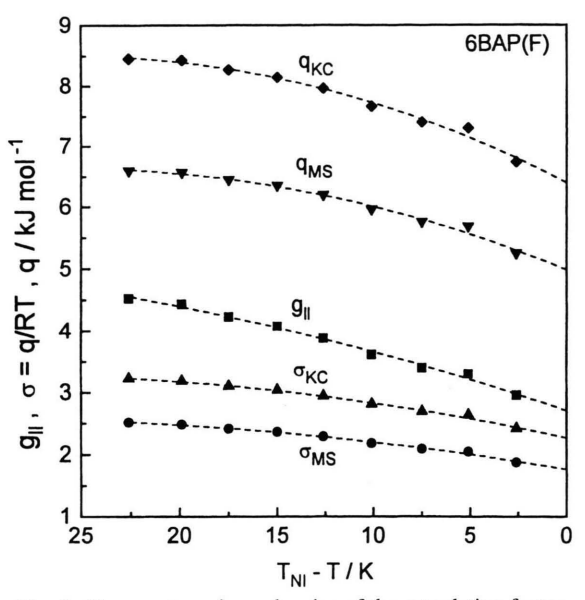


Fig. 6. Temperature dependencies of the retardation factor g_{\parallel} , the nematic potential barrier parameter σ according to (6), σ_{KC} , and (8), σ_{MS} , and the corresponding nematic potentials q_{KC} and q_{MS} .

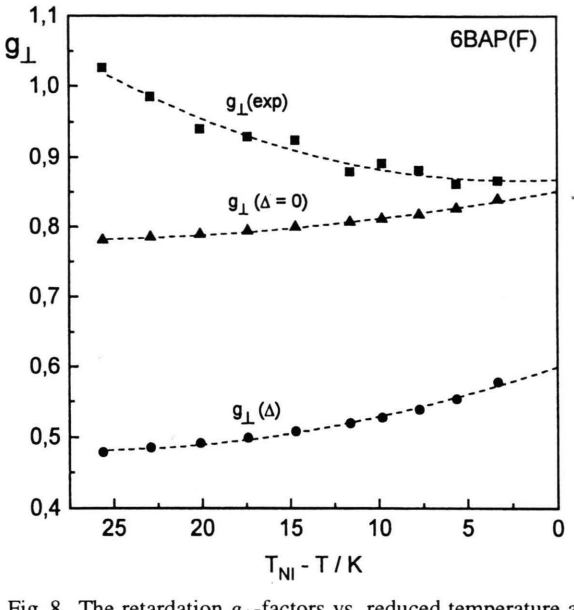


Fig. 8. The retardation g_{\perp} -factors vs. reduced temperature as calculated from the experimental data and from (7) (for details see text).

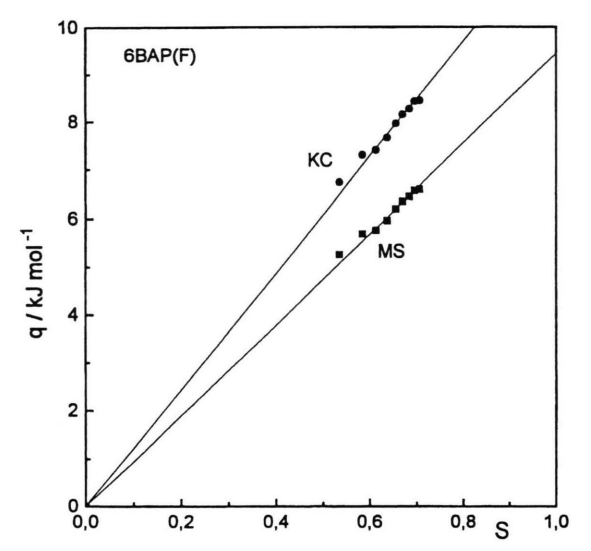


Fig. 7. Nematic potentials according to (6), KC, and (8), MS, vs. order parameter.

This gives $\mu_l/\mu_t \approx 0.40$ and $\beta \approx 68^\circ$. The simple vector addition under the assumption of a freely rotating –OCH₃ group results in $\mu_l/\mu_t \approx 0.48$ ($\beta \approx 64^\circ$); in this case the para – axis is regarded as molecular long axis, which is not likely, however. It seems reasonable to assume that

the dipole moment of the 6BAP(F) molecule is determined by the 3-fluoro-4-methoxyphenyl group, for which Minkin et al. [19] give the value $\mu = 2.31$ D. These quantities explain very well the observed dielectric anisotropy in the nematic phase of 6BAP(F).

As can be seen in Fig. 3, we have two sets of relaxation times characterizing the reorientations of molecules in the isotropic and nematic phase of 6BAP(F). τ_{\parallel} and τ_{\parallel} correspond to the reorientations around the short axes and are hindered by distinctly higher activation barriers than τ_{\perp} and τ_{\parallel} characterizing the rotations around the long axes (see Table 1). Additionally, at the Is-N transition point the first set of relaxation times undergoes a large jump, whereas the second one passes the clearing point rather smoothly (Figure 3). The ratio of the 1.f. relaxation times at $T_{\rm NI}$ is 2.9 for 6BAP(F) in comparison with 4.4 for 6BAPT [10]. The activation barriers for the molecular rotations around the short axes in both substances are comparable in the N phase, whereas they differ considerably in the Is phase.

In order to characterise the changes in the dynamics of molecules at the transition from the isotropic to the nematic phase, Meier and Saupe [1, 2] have introduced the so-called retardation factors defined as $g_{\parallel} = \tau_{\parallel}/\tau_0$ and $g_{\perp} = \tau_{\perp}/\tau_0$, where τ_0 is the relaxation time in the absence of the nematic potential. However, they assumed that τ_0

can be obtained by an extrapolation from the isotropic to the nematic phase of the so-called 'Debye relaxation time $\tau_{\rm D} = \xi/(2 kT)$ ' (ξ is the friction coefficient). The same interpretation of τ_0 is used in the theoretical papers by Coffey et al. [3, 4]. Usually the dielectric spectra of the isotropic phase of LC substances are broad due to the merging of two main relaxation processes, and τ_D is a mean value. In case of compounds with a strong longitudinal dipole moment (like cyanobiphenyls) it was proved that τ_D characterized mainly the rotations of molecules around the short axes [9]. This is due to the small contribution to the spectra from the perpendicular component of the dipole moment. In case of substances having comparable longitudinal and transverse dipole moments, the two motions should be well separated in the nematic as well as in the isotropic phase. This is really well seen in the case of the substance under study (Fig. 1) and leads to the definition of two retardation factors:

$$g_{\parallel} = \tau_{\parallel} / \tau_{01}, \qquad g_{\perp} = \tau_{\perp} / \tau_{0t},$$
 (5)

where τ_{01} and τ_{0t} are obtained by extrapolation from the iostropic to the nematic phase, as is shown in Figure 3. Thus, the above retardation factors characterize the same molecular motions with and without the nematic potential. Very recently, Kalmykov and Coffey [5] have generalized their former mean-field theory of the dielectric relaxation in the nematic phase to the case where μ is directed at an angle β to the molecular axis of symmetry [3, 4], They derived relationships between the above retardation factors and the nematic potential barrier parameter $\sigma = q/RT(g_{\parallel} \text{ case})$ or the order parameter $S(g_{\perp} \text{ case})$:

$$g_{11} = \frac{e^{\sigma} - 1}{\sigma} \left(\frac{2}{1 + 1/\sigma} \sqrt{\sigma/\pi} + 2^{-\sigma} \right)^{-1},$$
 (6)

$$g_{\perp} = \frac{(2-S)(1+\Delta)}{2+(2+S)\Delta - S/2},\tag{7}$$

where the parameter Δ is related to the rotational diffusion coefficients in the isotropic phase and may be expressed as $\Delta = (\tau_1/\tau_t - 1)/2$. Equation (6) consists of the well known Meier-Saupe [1, 2] formula

$$g_{11} = \frac{e^{\sigma} - 1}{\sigma} \tag{8}$$

with a correction term which causes that both formulas differ considerably for $\sigma > 1$ [3, 4]. We shall discuss these relationships, taking into account the present experimen-

Figure 6 presents the retardation factor g_{\parallel} , the σ -values calculated with the aid of (6) (σ_{KC}) and (8) (σ_{MS}) and the corresponding nematic potentials q_{KC} and q_{MS} , as functions of the reduced temperature $T_{NI} - T$. As can be seen the two formulae lead to quite different values of the nematic potential although they change similarly with the temperature. Taking into account the order parameter S from Fig. 5, we can check the relation between q and S. Figure 7 shows that the proportionality between them, predicted by Maier and Saupe [20], is fulfiled very well as in many other cases [7, 9]. The slopes v = q/S are: 12.1 kJ/mol (KC model) and 9.4 kJ/mol (MS model), and are close to that obtained for many cyanobiphenyl substances [7].

In our experiment the high frequency relaxation process is especially well established. Therefore it seems to us that we can verify (7). Figure 8 presents the experimental and calculated g_{\perp} – factors. In a first step we neglected the Δ -factor as in the original paper [5]. The calculated g_{\perp} – values are close to the experimental ones, although the temperature dependence is different. Next, the Δ -factors extrapolated from the isotropic to the nematic phase were taken into account (Δ changes roughly linearly between 15 and 24 within the N phase). In this case the difference is much more pronounced. The observed differences between the experimental and theoretical runs may partly be caused by too large S-values obtained from the optical studies.

Acknowledgement

Financial support of the Polish Government KBN Grant No 2 P03B 059 13 is gratefully acknowledged.

^[1] G. Meier and A. Saupe, Mol. Cryst. 1, 515 (1966).

^[2] A. J. Martin, G. Meier, and A. Saupe, Symp. Faraday Soc. **5,** 119 (1971).

^[3] W. T. Coffey, D. S. F. Crothers, Yu. P. Kalmykov, and J. T. Waldron, Physica A 213, 551 (1995).

^[4] W. T. Coffey, Yu. P. Kalmykov, and E. S. Massawe, Liq. Cryst. 18, 677 (1995).

^[5] Yu. P. Kalmykov and W. T. Coffey, Liq. Cryst. submitted.

^[6] H. Kresse, Adv. Liq. Cryst. 6, 109 (1981).[7] S. Urban, and A. Würflinger, Adv. Chem. Phys. 98, 143

^[8] S. Urban, B. Gestblom, H. Kresse, and R. Dabrowski, Z. Naturforsch. 51a, 834 (1996).

S. Urban, B. Gestblom, T. Brückert, and A. Würflinger, Z. Naturforsch. 50a, 984 (1995).

- [10] J. Jadżyn, C. Legrand, P. Kędziora, B. Żywucki, G. Cze-chowski, and D. Bauman, Z. Naturforsch. 51a, 933 (1996).
- [11] D. Bauman, P. Kedziora, C. Legrand, and J. Jadżyn, Liq. Cryst. 21, 389 (1996).
- [12] S. Urban, B. Gestblom, and R. Dabrowski, Liq. Cryst., in
- print.

 [13] R. Dabrowski, J. Dziaduszek, J. Szulc, K. Czupryński, and B. Sosnowska, Mol. Cryst. Liq. Cryst. 209, 201 (1991).

 [14] B. Gestblom, and S. Wróbel, Liq. Cryst. 18, 31 (1995).

 [15] W. H. de Jeu, Physical Properties of Liquid Crystaline
- Materials, Gordon & Breach, New York 1980, Chapt. 4.
- [16] R. G. Horn, J. Phys. Paris, 39, 105, 167 (1978); R. G. Horn, and T. E. Faber, Proc. Roy. Soc. A 368, 199 (1979).
- [17] M. L. Magnuson, B. M. Fung, and J. P. Bayle, Liq. Cryst. **19,** 823 (1995).
- [18] W. Maier and G. Meier, Z. Naturforsch. 16a, 262, 1200 (1961).
- [19] W. I. Minkin, O. A. Osipov, and Y. A. Zhdanov, Dipole Moments in Organic Chemistry, Plenum, New York 1970.
- [20] W. Maier and A. Saupe, Z. Naturforsch. 14a, 882 (1959); 15a, 287 (1960).